Mechanism of Ozone Decomposition on a Manganese Oxide Catalyst. 1. In Situ Raman Spectroscopy and Ab Initio Molecular Orbital Calculations

Wei Li,[†] G. V. Gibbs,[§] and S. Ted Oyama*[,‡]

Contribution from the Departments of Chemical Engineering, Chemistry, Geological Science, and Materials Science and Engineering, Virginia Polytechnic Institute and State University, Blacksburg, Virginia 24061-0211

Received April 27, 1998

Abstract: Ozone decomposition was investigated under reaction conditions by using Raman spectroscopy on a supported manganese oxide catalyst. An adsorbed species with a Raman signal at 884 cm^{-1} was observed during reaction, and was identified as a peroxide species by a combination of in situ Raman spectroscopy and ^{18}O isotopic substitution measurements. The observed isotope shift $\nu(^{18}O)/\nu(^{16}O)$ value of this adsorbed species was 0.946, in excellent agreement with the ratio calculated for a peroxide species (0.943) by using a harmonic oscillator model. Ab initio molecular orbital calculations confirmed this assignment, using $Mn(OH)_4(O_2)^+$ as a model compound for the adsorbed species. The reaction mechanism of ozone decomposition was elucidated with carefully designed experiments, including isotopic substitution. The reaction sequence involved dissociative adsorption of ozone to form an oxygen molecule and an atomic oxygen species, reaction of the atomic species with gaseous ozone to form an adsorbed peroxide species and gas-phase oxygen, and decomposition of the peroxide intermediate and desorption of molecular oxygen.

Introduction

Ozone decomposition is an environmentally significant reaction that has attracted considerable attention. While important work has been carried out in catalyst screening, fundamental studies on the reaction mechanism are lacking.[1] The objective of the present study is to investigate the nature of the adsorbed species formed from ozone so as to shed insight on the reaction mechanism. The observation, identification, and characterization of reaction intermediates are essential steps in understanding and establishing a reaction mechanism. This is the first paper of a pair in which we report a thorough investigation of the reaction intermediate during ozone decomposition on a manganese oxide catalyst. This paper covers identification of the reaction intermediate by use of in situ Raman spectroscopy, isotopic substitution, and theoretical calculations; the second paper describes the elucidation of the reaction mechanism from measurements of the steady-state and transient kinetic behavior of the observed reaction intermediate.

Using a silver oxide catalyst,[2] Imamura et al. suggested that negatively charged oxygen species were formed upon the introduction of ozone. Although a superoxide species was detected at 75 K by electron paramagnetic spectroscopy (EPR), its role in ozone decomposition reaction was not clearly determined. Naydenov, et al.[3] identified an O_3^- species on a CeO_2 surface, using EPR; however, they found that this species was not involved in the reaction. It was suggested that a highly reactive atomic oxygen species (probably O^-) might be the intermediate. However, prior to our work no direct observation of intermediates under reaction conditions has been accomplished with spectroscopic techniques.

There have been numerous studies of adsorbed oxygen species on oxides because of their key role in oxidation reactions.[4,5] EPR is a powerful technique for studying such species[6] yet has several limitations. For example, diamagnetic species such as O_2^{2-} and O^{2-} are not EPR-active; signals on paramagnetic oxides are usually too broad to resolve, owing to spin coupling; and in situ EPR measurements are difficult to implement[7] and give low signals at high temperatures. Infrared (IR) spectroscopy is another useful technique that has been widely used to study adsorbed species.[8] However, most oxide catalyst supports, i.e. alumina and silica, are very strong absorbers in the mid- and low-IR range (1000−100 cm^{-1}) where the vibrations of metal−oxygen bonds occur. Hence information on adsorbed species in that range is almost impossible to obtain. In contrast, Raman spectroscopy is uniquely suited to characterization of supported oxide catalysts because the weak scattering by the catalyst supports gives little interference. In recent years, advances in Raman instrumentation have significantly improved the throughput of Raman spectrometers, allowing studies of adsorbed species at low concentration. Recent work from the

* To whom correspondence should be addressed.
[†] Department of Chemical Engineering.
[‡] Departments of Chemical Engineering and Chemistry.
[§] Departments of Geological Science, Mathematics, and Materials Sciences and Engineering.

(1) Dhandapani, B.; Oyama, S. T. *Appl. Catal. B* **1997**, *11*, 129−166.
(2) Imamura, S.; Ikebata, M.; Ito, T.; Ogita, T. *Ind. Eng. Chem. Res.* **1991**, *30*, 217.
(3) Naydenov, A.; Stoyanova, R.; Mehandjiev, D. *J. Mol. Catal. A.* **1995**, *98*, 9.
(4) Che, M.; Tench, A. J. *Adv. Catal.* **1983**, *32*, 1−76.
(5) Che, M.; Tench, A. J. *Adv. Catal.* **1982**, *31*, 77−133.
(6) Lunsford, J. H. *Catal. Rev.* **1973**, *8*, 135−157.
(7) Che, M.; Giamello, E. in *Catalyst Characterization: Physical Techniques for Solid Materials*; Imelik, B.; Vedrine, J. C., Eds.; Plenum: New York, 1994.
(8) Davydov, A. A. *Infrared Spectroscopy of Adsorbed Species on the Surface of Transition Metal Oxides*, John Wiley: New York, 1984.

S0002-7863(98)01441-3 CCC: $15.00
Published on Web 08/22/1998

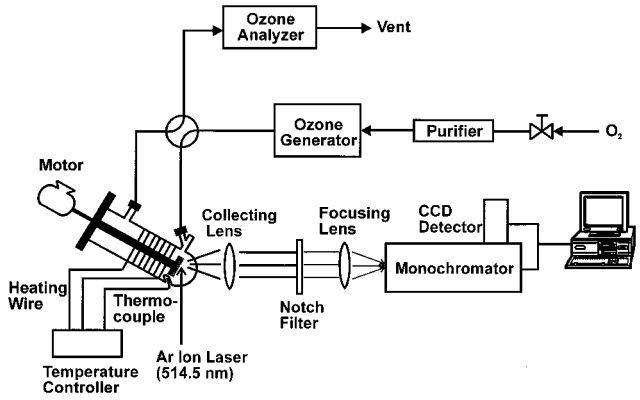

Figure 1. Schematic of the experimental setup for the in situ laser Raman experiments.

present group has demonstrated that in situ Raman spectroscopy is an excellent tool to study surface intermediates at reaction conditions.[9] In this paper, we apply this technique to the ozone decomposition reaction to directly observe and identify adsorbed intermediates, thereby gaining insight into the elementary steps of the reaction. We chose to study a supported manganese oxide catalyst because in previous work we found that easily reducible transition metal oxides, manganese oxide in particular, are good catalysts for ozone decomposition.[10]

Theoretical calculations using ab initio methods have undergone considerable progress in the past decade, owing to improvements in computational algorithms and advances in computer hardware. It is now possible, though still challenging, to obtain reliable vibrational frequencies, even for compounds involving transition metals,[11] with a fraction of the effort needed just a few years ago. Furthermore, the combination of experimental and theoretical approaches is particularly powerful for understanding and establishing reaction mechanisms.[12] In this paper, we report ab initio calculation results on several model manganese compounds to help identify the reaction intermediate observed during the ozone decomposition reaction.

Experimental Section and Computational Details

Catalyst Preparation. The 10 wt % MnO_2/Al_2O_3 used for this study was prepared by the incipient wetness impregnation method. Manganese acetate rather than nitrate was used as the precursor to improve the dispersion of manganese oxide on Al_2O_3.[13] $Mn(CH_3CO_2)_2 \cdot 4H_2O$ (Aldrich, >99.99%; 2.819 g) was dissolved in 9.6 cm^3 of distilled water, and the obtained solution was slowly added to 9.70 g of γ-Al_2O_3 (Aluminum Oxide C, Degussa; 94 $m^2\ g^{-1}$) while stirring. The sample was dried at 423 K and calcined at 773 K for 3 h. X-ray diffraction measurements did not show any features of manganese oxide, indicating that it was well-dispersed on the Al_2O_3 support. This agrees with the results of Kapteijn et al.[13], who, using manganese acetate as the precursor, showed that no crystalline manganese oxide phases on Al_2O_3 were observed for concentrations up to 8.4 wt % Mn.

In Situ Raman Spectroscopy. The schematic of the Raman apparatus shows the major components of the system (Figure 1). The excitation source was an Ar ion laser (Spex, Lexel 95) providing light with a wavelength of 514.5 nm and a power of 100 mW at the sample. A highly efficient holographic notch filter (Kaiser, Super Notch Plus) was used to remove the Raleigh line, thus allowing the use of a single-stage monochromator (Spex, 500M) rather than the conventionally used triple monochromator. A charge-coupled device (CCD; Spex, Spectrum One) cooled with liquid nitrogen was used as the detector. This setup offered a much higher throughput and allowed the observation and investigation of low-concentration reaction intermediates. A specially designed low-volume (<25 cm^3) in situ Raman cell enabled the spectrum to be acquired under conditions of controlled temperature and pressure in a flow of reactant stream. The catalyst was pressed into a thin wafer ~1 mm thick with a diameter of 15 mm and was held by a stainless steel cap on a ceramic rod, which was spun at 1000 rpm to avoid sample overheating. The temperature of the sample was measured by a thermocouple installed in a well 3 mm from the sample wafer. The Raman spectroscopic measurements were carried out at room temperature, except where specified, and atmospheric pressure. The Raman spectrometer had a resolution of ~6 cm^{-1}. For the isotope substitution experiments, a specially designed setup was used.[14] Two gas containers isolated with Teflon stopcocks were used to store $^{16}O_2$ (Airco, >99.6%) and $^{18}O_2$ (Isotec, >99 at. %), from which ozone was generated by discharging a Tesla coil. The produced ozone/oxygen mixture (^{18}O or ^{16}O or a combination of both) could be introduced into the Raman cell separately or together. The Raman cell and the gas containers were evacuated prior to the gas dosing. In other experiments, ozone was produced by passing $^{16}O_2$ through a high-voltage silent-discharge ozone generator (OREC, V5−0). Prior to the Raman spectroscopic measurements, the samples were pretreated with flowing oxygen at 773 K for 3 h.

Calculation Details. All calculations were performed with a GAUSSIAN 94 program.[15] The geometry optimization of manganese model compounds $Mn(OH)_4(O_2)^+$ and MnO_3OH was carried out by using the Hartree−Fock method and a 6-311G triple-ζ basis set with all electrons treated explicitly; the vibrational frequencies of the compounds were computed by determining the second derivatives of the energy. The raw calculated frequency values at the Hartree−Fock level contain known systematic errors due to the neglect of electron correlation, resulting in overestimates of ~10−12%. Hence we followed standard practice and scaled the predicted frequencies by an empirical factor of 0.8929[16] before reporting them here. The oxidation state of manganese in the model compounds was chosen to be +7, given the likelihood that high-valency compounds would be found in the presence of the strongly oxidizing ozone.[17]

Results

Raman Spectra of Adsorbed Species. The Raman spectra of the catalyst sample were compared under oxygen and an ozone/oxygen mixture at room temperature (Figure 2). The spectrum under pure oxygen (Figure 2a) exhibited a peak at 654 cm^{-1}. Exposing the catalyst sample to an ozone/oxygen mixture produced two changes in the Raman spectrum (Figure 2b): a sharp new peak at 884 cm^{-1}, and a decrease in intensity and broadening of the peak at 654 cm^{-1}. The peak at 884 cm^{-1} was accompanied by two very weak peaks at 930 and 954 cm^{-1}. The appearance of the new peak was reversible; i.e., it disappeared after ozone was purged. However, the intensity decrease of the 654 cm^{-1} peak was not reversed upon removal

(9) (a) Zhang, W.; Oyama, S. T. *J. Phys. Chem.* **1996**, *100*, 10759−10767. (b) Zhang, W.; Oyama, S. T. *J. Am. Chem. Soc.* **1996**, *118*, 7173−7177.

(10) Dhandapani, B.; Oyama, S. T. *Chem. Lett.* **1995**, 413−414.

(11) (a) Scott, A.; Radom, L. *J. Phys. Chem.* **1996**, *100*, 16502−16513. (b) Head, J. D. *Int. J. Quantum Chem.* **1997**, *65*, 827−838.

(12) (a) Lee, D. G.; Moylan, C. R.; Hayashi, T.; Brauman, J. I. *J. Am. Chem. Soc.* **1987**, *109*, 3003−3010. (b) Nakai, H.; Ohmori, Y.; Nakatsuji, H. *J. Phys. Chem.* **1995**, *99*, 8550−8555.

(13) Kapteijn, F.; Langeveld, A. D.; Moulijn, J. A.; Andreini, A.; Vuurman, M. A.; Turek, A. M.; Jehng, J. M.; Wachs, I. E. *J. Catal.* **1994,** *150*, 94−104.

(14) Li, W. Ph.D. Dissertation, Virginia Tech, Blacksburg, 1998.

(15) Frisch, M. J.; Trucks G. W.; Schlegel, H. B.; Gill, P. M. W.; Johnson, B. G.; Robb, M. A.; Cheeseman, J. R.; Keith, T. A.; Peterson, G. A.; Montgomery, J. A.; Raghavachai, K.; Al-Laham, M. A.; Zakrzewski, V. G.; Ortiz, J. V.; Foresman, J. B.; Cioslowski, J.; Stefanov, B. R.; Nanayakkara, A.; Challacombe, M.; Peng, C. Y.; Ayala, P. Y.; Chen, W.; Wong, M. W.; Andres, J. L.; Replogle, E. S.; Gomperts, R.; Martin, R. L.; Fox, D. J.; Binkley, J. S.; Defrees, D. J.; Baker, J.; Stewart, J. P.; Head-Gordon, M.; Gonzales, C.; Pople, J. A. *GAUSSIAN 94* (revision C.2), Gaussian: Pittsburgh, 1995.

(16) (a) Pople, J. A.; Krishnan, R.; Schlegel, H. B.; DeFrees, D.; Binkley, J. S.; Frisch, M. J.; Whiteside, R. F.; Hout, R. F.; Hehre, W. J. *Int. J. Quantum Chem., Symp.* **1981**, *15*, 269. (b) Cundari, T.; Raby, P. *J. Phys. Chem. A* **1997**, *101*, 5783−5788.

(17) *Gmelin's Handbook of Inorganic Chemistry* 1973; Vol. MnCl, pp. 300.

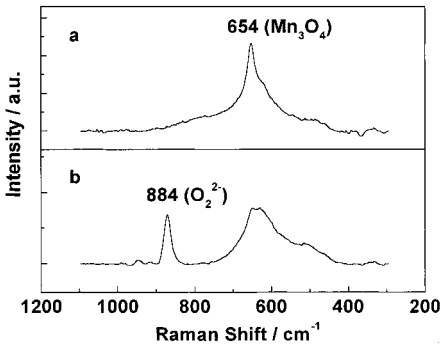

Figure 2. In situ Raman spectra of the catalyst sample: (a) in oxygen; (b) in a 2 mol % ozone/oxygen mixture. Reactant flow rate = 1000 cm^3 min^{-1} at room temperature. Spectrum acquisition conditions (Figures 2 and 3): laser power = 100 mW, resolution = 6 cm^{-1}, exposure time = 30 s. n = 60 scans.

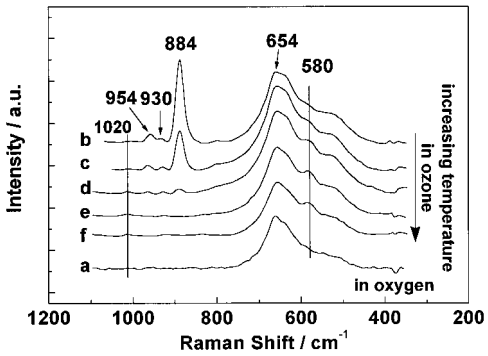

Figure 3. In situ Raman spectra of the catalyst sample in a 2 mol % ozone/oxygen mixture (except a) at various temperatures: (a) 293 K in pure oxygen; (b) 293 K; (c) 323 K; (d) 373 K; (e) 423 K; (f) 473 K. Reactant flow rate = 1000 cm^3 min^{-1}. n = 60 scans.

of ozone and could be restored only by subsequent treatment in oxygen at elevated temperature (773 K). An interesting feature of the new signal at 884 cm^{-1} was that, in addition to the fundamental vibration mode, the first and second overtones were also visible at 1754 and 2618 cm^{-1}, respectively (not shown). In the course of these measurements, the ozone continuously underwent decomposition. The kinetics of this process will be treated in depth in the companion paper.

We also studied the effect of temperature on the in situ Raman spectrum. The intensity of the signal at 884 cm^{-1} decreased significantly with increasing temperature (Figure 3), and the signal eventually disappeared completely at ~423 K. Meanwhile, a new peak at 580 cm^{-1} increased in intensity with increasing temperature up to 423 K, then decreased slightly in intensity with further increases in temperature. A very weak signal at 1020 cm^{-1} also appeared at higher temperatures (>373 K).

Isotopic Substitution. When ozone was generated by using $^{18}O_2$ rather than $^{16}O_2$, the signal at 884 cm^{-1} shifted to 834 cm^{-1}, and the first overtone at 1746 cm^{-1} also shifted, to 1670 cm^{-1} (Figure 4). The ratio of $\nu(^{18}O)/\nu(^{16}O)$ was calculated to be 0.946. The peak at 1556 cm^{-1} can be assigned to gas phase $^{16}O_2$, while the peak at 1468 cm^{-1} can be assigned[18] to gas phase $^{18}O_2$. Since ozone was produced by discharging a Tesla coil for the isotopic substitution experiments, its concentration was much lower than when ozone was produced by the ozone generator via corona discharge; hence we saw no attenuation of the peak at 662 cm^{-1}.

(18) Selig, H.; Claassen, H. H. *Israel J. Chem.* **1968**, *6*, 499−500.

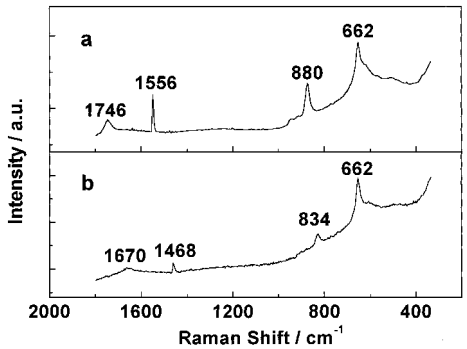

Figure 4. In situ Raman spectra of the catalyst sample after ozone adsorption: (a) in $^{16}O_3/^{16}O_2$; (b) in $^{18}O_3/^{18}O_2$. Static condition at room temperature. Spectrum acquisition conditions (Figures 4−6): laser power = 100 mW, resolution = 6 cm^{-1}, exposure time = 30 s.

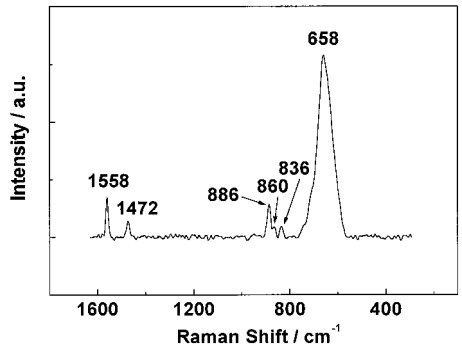

Figure 5. In situ Raman spectra of the catalyst sample in a mixture of $^{16}O_3/^{16}O_2$ and $^{18}O_3/^{18}O_2$. Static condition at room temperature.

To explore the origin of oxygen atoms in the adsorbed species, we also measured the in situ Raman spectra of the sample after the surface was exchanged with $^{18}O_2$. The ^{18}O-exchanged catalyst surface was obtained by repeated reduction in H_2 at 623 K for 1 h followed by oxidation in $^{18}O_2$ at 623 K for 1 h. The reduction and oxidation temperature, determined from a temperature-programmed reduction profile of the catalyst sample, was chosen to be a temperature just below that at which the bulk sample was reduced. The bulk Raman spectrum of the ^{18}O-exchanged surface showed no difference from that of the unexchanged surface. The Raman spectra with $^{16}O_3$ and $^{18}O_3$ also exhibited no differences from those on the unexchanged surface.

When a mixture of $^{16}O_3$ and $^{18}O_3$ without mixed isotopes ($^{16}O_2{}^{18}O$, $^{16}O^{18}O_2$) was decomposed, three peaks were observed, at 886, 860, and 836 cm^{-1} (Figure 5). The mixture was formed by combining $^{16}O_3/^{16}O_2$ and $^{18}O_3/^{18}O_2$, which had been separately prepared by discharging a Tesla coil in $^{16}O_2$ and $^{18}O_2$, respectively.

Sequential Raman measurements were also carried out. The catalyst sample was first exposed to a mixture of $^{18}O_3/^{18}O_2$; then, after a brief purging with helium, an $^{16}O_3/^{16}O_2$ mixture was introduced. The resulting Raman spectrum exhibited only two peaks, at 856 and 882 cm^{-1} (Figure 6).

Ab Initio Calculations of Model Mn Compounds. Model calculations were completed on MnO_3OH and $Mn(OH)_4(O_2)^+$, for reasons to be discussed later. The optimized geometries are shown in Figure 7. The optimized structure of MnO_3OH has C_s point symmetry, whereas that of $Mn(OH)_4(O_2)^+$ has C_{2v} symmetry. The GAUSSIAN program also calculates the peak intensity of IR and Raman spectra, though only the order of intensity rather than the absolute values is reliable. We present here only the vibrational frequencies with a significant Raman

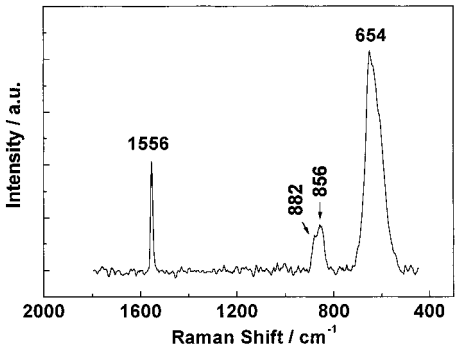

Figure 6. In situ Raman spectra of the catalyst sample after a sequential adsorption of ozone. The catalyst sample was first exposed to an $^{18}O_3/^{18}O_2$ mixture. Then, after a brief purging with helium, an $^{16}O_3/^{16}O_2$ mixture was introduced. Static condition at room temperature.

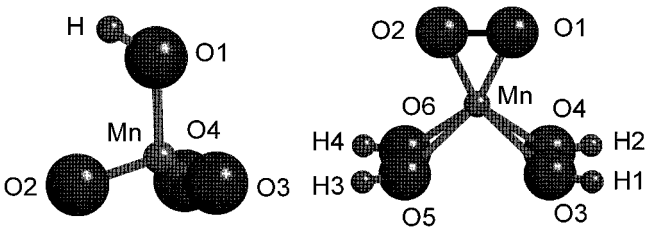

Figure 7. Optimized structure of manganese model compounds determined with the Hartree−Fock method and a 6-311G triple-ζ basis set: (left) MnO_3OH, C_s symmetry. Selected bond lengths and angles: Mn−O1 0.176 nm, Mn−O2 0.156 nm, O1−Mn−O2 105.4°, O2−Mn−O3 111.7°. (right) $Mn(O_2)(OH)_4^+$, C_{2v} symmetry. Selected bond lengths and angles: Mn−O1 0.176 nm, Mn−O3 0.212 nm, O1−O2 0.146 nm, O3−O4 0.144 nm, O3−O5 0.302 nm, O1−Mn−O2 49.3°.

Table 1. Selected Vibrational Frequencies of ^{18}O-Substituted $Mn(OH)_4(O_2)^+$

compound	ν, cm^{-1}	compound	ν, cm^{-1}
$Mn(^{16}O_2)(^{16}OH)_4^+$	899	$Mn(^{16}O^{18}O)(^{16}OH)_4^+$	876
$Mn(^{18}O_2)(^{16}OH)_4^+$	852	$Mn(^{16}O_2)(^{18}OH)_4^+$	899

Table 2. Selected Vibrational Frequencies of ^{18}O-Substituted MnO_3OH

compound	ν, cm^{-1}
$Mn^{16}O_3{}^{16}OH$	859,[a] 938, 1020
$Mn^{18}O^{16}O_2{}^{16}OH$	855, 915, 1002
$Mn^{16}O^{18}O_2{}^{16}OH$	852, 901, 976
$Mn^{18}O_3{}^{16}OH$	832,[a] 901, 969

[a] $\nu(^{18}O)/\nu(^{16}O) = 0.969$.

intensity. Both complexes have Raman signals [$Mn(OH)_4(O_2)^+$ at 899 cm^{-1}, and MnO_3OH at 859 cm^{-1}] positioned close to the observed signal of the adsorbed species, suggesting that criteria other than the frequency value should be used to distinguish between the two model complexes. We also calculated vibrational frequencies of isotopically substituted complexes of $Mn(OH)_4(O_2)^+$ (Table 1) and MnO_3OH (Table 2) to determine the isotope shift of these two Raman signals. The O−O stretching in $Mn(OH)_4(O_2)^+$ exhibited an isotopic shift of 47 cm^{-1}, corresponding to a $\nu(^{18}O)/\nu(^{16}O)$ value of 0.948, while in MnO_3OH the $\nu(^{18}O)/\nu(^{16}O)$ value was 0.969. However, the frequency value of the O−O stretching mode in $Mn(OH)_4(O_2)^+$ did not change when the oxygen atoms in the hydroxyl groups were replaced with ^{18}O, suggesting that this vibrational mode is highly localized.

An unusual feature in the optimized structure of $Mn(OH)_4(O_2)^+$ is that the two neighboring oxygen atoms in the hydroxyl groups are very close (0.1437 nm) to one another, suggesting there may be interactions between the hydroxyl groups. The reason for this is still unknown, but addition of polarized and diffuse functions to the basis set resulted in a collapse of the complex.

Discussion

Raman Spectra of the Adsorbed Species. Given the dark color of the manganese sample (deep brown), the Raman spectra should be considered mainly as indicative of near-surface phases. The peak at 654 cm^{-1} can be ascribed to Mn_3O_4.[13] However, this observation does not rule out the presence of other phases because MnO_2 is Raman-inactive, whereas Mn_2O_3 and MnO show only very weak Raman signals. The intensity decrease of the Mn_3O_4 signal upon exposure to ozone indicates that the dispersed manganese oxide is partially oxidized by ozone. Also, this oxidation seems to be irreversible since the peak intensity is not recovered even after the ozone is purged.

The new signal at 884 cm^{-1} suggests that a new species has been formed on the catalyst surface during the ozone decomposition reaction. The possibility that this signal was due to a gas-phase species was ruled out with blank experiments in the absence of the catalyst. This is the first case of direct spectroscopic detection of an adsorbed species during ozone decomposition. The signal at 884 cm^{-1} can be assigned to an adsorbed peroxide species, as discussed in detail in the next section. The fact that its overtones were also observed suggests that this signal could be resonance-enhanced. This is not unusual; resonance Raman spectra of several manganese oxo compounds[19] [e.g., MnO_4^-, MnO_3F, Mn(*TPP*)O_2, Mn(*TTP*)O_2] have been reported.

New signals at 580 and 1020 cm^{-1} are probably related to atomic oxygen species (Figure 3). That they are detectable even at temperatures >373 K suggests a higher thermal stability of the atomic oxygen species than of the molecular oxygen species.

Assignment of the Adsorbed Species. Definitive identification of an adsorbed species is almost always a very difficult task, but obtaining results by using more than one technique can improve the reliability of the assignment. For this observed adsorbed species, we combined vibrational frequency measurements of the unsubstituted and ^{18}O-substituted species with ab initio calculations to select from several possible candidates.

The characteristic vibrational frequencies of adsorbed oxygen species have been summarized in a review.[4] Several species, including Mn═O, Mn−O−Mn, and O_2^{2-}, can be considered possibilities. Also a recent study on MnO_3F[20] reported that its Raman spectrum has a signal at 886 cm^{-1}. Because F was not present in our system, it was replaced by OH and calculations were completed on the model compound MnO_3OH, for which calculations show that the Mn═O vibration does not change with the substitution for F by OH.

Although peroxide and Mn−O−Mn species have similar frequencies,[5] the thermal stability of the peroxide species is usually much lower than that of the Mn−O−Mn species.[21] The observed adsorbed species disappeared when the temperature was raised to ∼423 K, suggesting that the observed signal is more likely to be from a molecularly adsorbed oxygen than from the Mn−O−Mn group.

(19) (a) Weselucha-Birczynska, A.; Proniewicz, L. M.; Bajdor, K.; Nakamoto, K. *J. Raman Spectrosc.* **1991**, *22*, 315−319. (b) Kiefer, W.; Bernstein, H. J. *Chem. Phys. Lett.* **1971**, *8*, 381−383. (c) Czernuszewicz, R. S.; Su, Y. O.; Stern, M. K.; Macor, K. A.; Kim, D.; Groves, J. T.; Spiro, T. G. *J. Am. Chem. Soc.* **1988**, *110*, 4158−4165. (d) Nick, R. J.; Ray, G. B.; Fish, K. M.; Spiro, T. G.; Groves, J. T. *J. Am. Chem. Soc.* **1991**, *113*, 1838−1840.

(20) Varetti, E. L. *J. Raman Spectrosc.* **1991**, *22*, 307−309.

Table 3. Isotopic Shifts (O^{18}/O^{16})

	^{18}O substitution		
	single	double	triple
Mn═O	0.956		
O−O	0.972	0.943	
MnO_3OH	0.976	0.964	0.955
observed		0.946	

Ozonide (O_3^-) species have also been reported for ozone adsorption on oxide surfaces[22] as well as in matrix isolation reactions of ozone with alkali and alkali earth metals.[23] The signals of the ozonide species were usually in the range of 800−900 cm^{-1}, but those measurements were carried out at very low temperatures (<100 K), and such adsorbed ozonide species quickly disappear with increasing temperature.[22] Hence the species we observed is unlikely to be an ozonide species.

Isotopic Substitution Experiments. The isotope shifts of the observed species and those of the several possible candidates are listed in Table 3. The shift is expressed as the ratio of the vibrational frequency of the ^{18}O substituted species and that of the unsubstituted species, $\nu(^{18}O)/\nu(^{16}O)$. Since more than one oxygen atom is present in some species, the shifts caused by ^{18}O substitution of one, two, and three oxygen atoms are listed (in columns 2, 3, and 4, respectively). For Mn═O and O_2^{2-} species, a harmonic diatomic model is assumed. The isotope shift of the observed species (0.946) is very close to that of a peroxide species (0.943), indicating that the observed species can be assigned to a peroxide species.

Peroxide species have been reported on various oxide catalysts. Onishi and co-workers, using Fourier transform-IR, identified a peroxide species with a vibrational frequency of 883 cm^{-1} on a partially reduced CeO_2 surface.[24] Lunsford and co-workers, in carrying out an in situ Raman study of oxidative coupling catalysts,[25] observed a surface peroxide species with a Raman signal at 863 cm^{-1} and discussed its role in methane activation. Lunsford et al.[26] and Su and Bell[27] also detected surface peroxide species on Ba/MgO catalysts. The spectrum of the peroxide species was characterized by a major line at 842 cm^{-1}, with minor peaks at 829 and 821 cm^{-1}. Also for ozone decomposition, a negatively charged species was suggested as the reaction intermediate,[2,10] in agreement with the present work.

Ab Initio Calculations of Model Mn Compounds. Calculations on several manganese model compounds indicate that the methodology we used is able to generate reliable geometry and vibrational frequencies of manganese compounds. We found that a peroxide complex $Mn(OH)_4(O_2)^+$ can serve as an appropriate model for the observed adsorbed species. Both the calculated vibrational frequency (899 cm^{-1}) and the calculated isotope shift $\nu(^{18}O)/\nu(^{16}O)$ value (0.948) are in excellent agreement with the experimental values (884 cm^{-1} and 0.946). This strengthens our assignment of this adsorbed species as a peroxide complex.

For MnO_3OH, the Raman signal lies in the range where the adsorbed species was observed, but the isotopic shift (0.969) does not match. In addition, it is very unlikely that all three terminal oxygen will have originated from the ozone molecule. If there is partial mixing with surface ^{16}O, the isotopic shift will be even farther from the observed value.

Manganese Peroxide Complexes. Manganese dioxygen complexes have attracted considerable interest because of their suggested roles in important enzymatic reactions such as superoxide dismutation and photosynthesis reactions.[28] Four manganese peroxide compounds have been structurally determined and characterized: a monomeric side-on Mn(III) porphyrin compound, $Mn^{III}(TPP)(O_2)^-$ [29], a binuclear (μ-peroxo)dimanganese(IV) complex, $[L_2Mn_2(\mu\text{-}O)_2(\mu\text{-}O_2)](ClO_4)_2$ (L = 1,4,7-trimethyl-1,4,7-triazacyclononane), a trinuclear (μ_3-oxo, μ-peroxo) Mn(III) complex;[30] and a monomeric side-on peroxo manganese(III) complex, $Mn(O_2)(3,5\text{-}iPr_2pzH)(HB(3,5\text{-}iPr_2pz)_3)$.[31] In all these complexes the peroxo species adopts a side-on geometry with O−O distances from 0.142 to 0.146 nm, consistent with that of our peroxide model $Mn(OH)_4(O_2)^+$. However, the highest oxidation state of manganese in these complexes is +4 in contrast to +7 in the model compound. No information is available in the literature for the dependence of O−O bond length on the oxidation state of manganese, given the limited number of structurally characterized manganese peroxide compounds. However, the bond length of Mn−O was found not to be affected by the oxidation state of manganese.[32] The vibrational frequencies of the O−O stretching in these complexes vary from 812 to 990 cm^{-1}, also in agreement with those observed and calculated for the peroxide species in this work. As mentioned earlier, the oxidation state of manganese was chosen to be +7 because of the extremely strong oxidizing ability of ozone. Manganese compounds in such higher oxidation states are usually unstable and decompose to release oxygen,[19] which suggests that the optimized geometry of the peroxide species probably corresponds to a local minimum with a very shallow potential well. This is in agreement with the characteristics of the adsorbed species we observed: This adsorbed species is observed only in the presence of ozone and gradually disappears when ozone is removed.

Reaction Chemistry. From the results of this investigation, we deduced that ozone adsorbs to form a peroxide intermediate. When a mixture of $^{16}O_3$ and $^{18}O_3$ with no ozone of mixed isotopes ($^{16}O_2{}^{18}O$, $^{16}O^{18}O_2$) was decomposed, three peaks corresponding to the peroxide species $^{16}O_2$, $^{16}O^{18}O$, and $^{18}O_2$ were observed (Figure 5), indicating that the peroxide species was formed through atomic oxygen species. Hence ozone adsorption to form the peroxide species can be described by

$$O_3 + * \rightarrow O_2 + O^* \quad (1)$$

$$O^* + O_3 \rightarrow O_2 + O_2^* \quad (2)$$

Here the symbol * represents a surface site. When the catalyst is brought into contact with ozone, its surface is quickly

(21) Onishi, T. in *Dynamic Processes on Solid Surfaces*; Tamaru, K., Ed.; Plenum: New York, 1994; pp. 237−259.
(22) Bulanin, K. M.; Lavalley, J. C.; Tsyganenko, A. A. *J. Phys. Chem. B* **1997**, *101*, 2917−2922.
(23) (a) Spiker, R. C.; Andrews, L. *J. Chem. Phys.* **1973**, *59*, 1851−1862. (b) Andrews, L.; Spiker, R. C. *J. Chem. Phys.* **1973**, *59*, 1863−1871. (c) Jacox, M. E.; Milligan, D. E. *J. Mol. Spectrosc.* **1972**, *43*, 148−167.
(24) Li, C.; Domen, K.; Maruya, K.; Onishi, T. *J. Am. Chem. Soc.* **1989**, *111*, 7683.
(25) Mestl, G.; Knözinger, H.; Lunsford, J. H. *Bunsen-Ges. Phys. Chem.* **1993**, *97*, 319.
(26) Lunsford, J. H.; Yang, X.; Haller, K.; Mestl, L. G.; Knözinger, H. *J. Phys. Chem.* **1993**, *97*, 13810.
(27) Su, S. C.; Bell, A. T. *Catal. Lett.* **1996**, *36*, 15.
(28) Pecoraro, V. L.; Baldwin, M. J.; Gelasco, A. *Chem. Rev.* **1994**, *94*, 807−826.
(29) VanAtta, R. B.; Strouse, C. E.; Hanson, L. K.; Valentine, J. S. *J. Am. Chem. Soc.* **1987**, *109*, 1425−1434.
(30) Bhula, R.; Gainsford, G. J.; Weatherburn, D. C. *J. Am. Chem. Soc.* **1988**, *110*, 7550−7552.
(31) Kitajima, N.; Komatsuzaki, H.; Hikichi, S.; Osawa, M.; Moro-oka, Y. *J. Am. Chem. Soc.* **1994**, *116*, 11596−11597.
(32) Palenik, G. J. *Inorg. Chem.* **1997**, *36*, 4888−4890.

covered by atomic oxygen species through dissociative adsorption of ozone, and a Rideal−Eley type reaction of a gaseous ozone molecule with a surface atomic oxygen occurs to form an adsorbed peroxide species and a gaseous oxygen molecule. Another possible route for converting the atomic oxygen species to the peroxide species is through a bimolecular surface reaction:

$$2O^* \rightarrow O_2^* + * \quad (3)$$

However, because no Raman signals attributable to $^{18}O_2^{2-}$ species were observed after the sequential introduction of $^{16}O_3$ after $^{18}O_3$, this process is ruled out (Figure 6). Also, the fact that the Raman signal for $^{16}O^{18}O^{2-}$ species was observed after the sequential introduction of $^{16}O_3$ after $^{18}O_3$ indicates that step 2 is much slower than step 1.

When ozone is removed from the gas phase, the intensity of the surface peroxide signal decreases gradually with time. This suggests that the final step in the ozone decomposition reaction is a slow decomposition of the peroxide species to form gaseous oxygen.

$$O_2^* \xrightarrow{\text{slow}} O_2 + * \quad (4)$$

In summary, ozone adsorbs dissociatively on the catalyst surface to form an oxygen molecule and an atomic oxygen species. The atomic species reacts with another gaseous ozone to form a peroxide species and a gas-phase oxygen molecule. The adsorbed peroxide species, the most abundant reaction intermediate, decomposes to form a gas-phase oxygen molecule. This mechanism explains why transition metal oxides such as manganese oxides, which have easily accessible multiple oxidation states, are good catalysts for ozone decomposition. The mechanism consists mainly of redox steps: adsorption of ozone on the catalyst, and desorption of the adsorbed intermediates. At steady state, the rates of these steps are equal. Consequently, the faster the catalyst undergoes oxidation and reduction, the faster will be the rate of the decomposition reaction.

Conclusions

Ozone decomposition was investigated under reaction conditions by using Raman spectroscopy on a supported manganese oxide catalyst. An adsorbed species with a Raman signal at 884 cm^{-1} was observed during reaction, and this species was assigned to a peroxide species on the basis of the results for a combination of in situ Raman spectroscopy and ^{18}O isotopic substitution. The observed isotope shift $\nu(^{18}O)/\nu(^{16}O)$ value of this adsorbed species was 0.946, in excellent agreement with the ratio expected for a peroxide species (0.943). Theoretical calculations with a Hartree−Fock method confirmed this assignment, and $Mn(OH)_4(O_2)^+$ was found to be a good model compound for the adsorbed species.

The reaction steps in ozone decomposition were elucidated with carefully designed experiments that used isotopic substitution. The reaction was determined to consist of dissociative adsorption of ozone to form an oxygen molecule and an atomic oxygen species, reaction of the atomic species with gaseous ozone molecule to form an adsorbed peroxide species and gas-phase oxygen, and decomposition of the peroxide intermediate and desorption of molecular oxygen. This reaction sequence will be treated in the companion paper through use of transient and steady-state kinetic measurements of the ozone decomposition reaction and the adsorbed peroxide intermediate.

$$O_3 + * \rightarrow O^* + O_2 \quad (5)$$

$$O_3 + O^* \rightarrow O_2^* + O_2 \quad (6)$$

$$O_2^* \rightarrow O_2 + * \quad (7)$$

Acknowledgment. We gratefully acknowledge the financial support for this work by the Director, Division of Chemical and Thermal Systems of the National Science Foundation, under Grant CTS-9712047. We thank Joseph Merola for valuable comments on the reaction mechanism.

JA981441+